

Direct Observation of Biaxial Confinement of a Semiflexible Filament in a Channel

M. C. Choi,^{†,‡} C. D. Santangelo,[§] O. Pelletier,[‡]
J. H. Kim,[†] S. Y. Kwon,^{†,‡} Z. Wen,^{||} Y. Li,[‡]
P. A. Pincus,^{†,‡} C. R. Safinya,[‡] and M. W. Kim^{*,†,‡}

Department of Physics, Korea Advanced Institute of Science and Technology, Daejeon 305-701, Korea, Materials Research Laboratory and Department of Materials, Physics, Molecular, Cellular, and Developmental Biology, University of California—Santa Barbara, Santa Barbara, California 93106, Department of Physics and Astronomy, University of Pennsylvania, Philadelphia, Pennsylvania 19101, College of Optoelectronic Engineering, Chongqing University, Chongqing, China, and Temperature-Humidity Group, Korea Research Institute of Standards and Science, Daejeon, Korea

Received June 24, 2005

Revised Manuscript Received August 24, 2005

Actin is a key component of the protein complex responsible for producing contractile force in skeletal muscle. It is highly enriched near the cell surface in nonmuscle cells and plays an important role in both a cell's shape deformations and response to mechanical stress.^{1–4} Filamentous actin, called F-actin, is a two-stranded helical protofilament with a diameter of ~ 80 Å and a contour length of ~ 10 μm . The experimental results show that the persistence length L_p of F-actin is 4–20 μm .^{5–8} One of interesting experiments is to find the statistics and behaviors of a semiflexible filament in a confined space, such as a channel width $W \leq L_p$,⁹ which has in fact never been reported before. Because the persistence length of F-actin is long enough to be visualized in situ by video fluorescence microscopy, actin is an ideal system for this study.

The tangent-tangent correlation function $\langle C(s) \rangle$ is defined as

$$\langle C(s) \rangle = \langle \vec{u}(0) \cdot \vec{u}(s) \rangle = \langle \cos[\theta(s) - \theta(0)] \rangle \quad (1)$$

where s is the arclength along the chain, $\vec{u}(s)$ the unit tangent vector along s , and θ the angle measured from the channel axes (see Figure 1a). The persistence length is the characteristic distance along the chain at which the unit vector $\vec{u}(s)$ becomes uncorrelated. For a semiflexible polymer in two-dimensional free space,

$$\langle C(s) \rangle \sim e^{-s/2L_p} \quad (2)$$

The persistence length is intrinsic to the chain and is determined, for example, by buffer and polymerization conditions.⁸ In particular, it is constant for an unconfined chain in two dimensions, independent of the contour length of the chain. For a polymer confined to a channel, however, this definition is not applicable

* Author to whom correspondence should be addressed. E-mail address: mwkim@kaist.ac.kr.

[†] Department of Physics, Korea Advanced Institute of Science and Technology.

[‡] Materials Research Laboratory and Department of Materials, Physics, Molecular, Cellular, and Developmental Biology, University of California—Santa Barbara.

[§] Department of Physics and Astronomy, University of Pennsylvania.

^{||} College of Optoelectronic Engineering, Chongqing University.

[‡] Temperature-Humidity Group, Korea Research Institute of Standards and Science.

because $\langle C(s) \rangle$ does not generically decay exponentially. In this letter, we ask whether we can define a new length scale, the effective persistence length L_p^{eff} , which is determined by the geometrical constraints on the chain configurations due to confinement.

Alexa-488-labeled globular (G-) actin was suspended in a standard buffer solution.¹⁰ Polymerization was carried out mainly with 100 mM KCl and the addition of phalloidin to stabilize the filaments. Microchannels with a depth of 1 μm and widths of 3, 5, 10, and 20 μm , were fabricated on Si substrates using photolithography and reactive ion etching. To prevent the F-actin solution from evaporating, the channels were sealed with a water-insoluble oil, as shown in the cartoon Figure 1b. A single channel was filled with 2 $\mu\text{g/mL}$ of F-actin solution through a glass capillary tube using a microinjector.^{11–12}

To investigate the thermal fluctuations of a F-actin in a channel, we used a high-resolution video microscopy system, composed of an optical microscope and a silicon-intensified target (SIT) camera VE1000.¹³ At room temperature, a single chain of F-actin undergoes fluctuations with characteristic time scales of seconds. The F-actin fluctuations were recorded using video microscopy and then were captured by a frame grabber. F-actin in the fluorescence images (Figure 1c) has a thickness of ~ 1 μm and a contour length of ~ 18 μm .

The confinement effect is not conspicuously observed in the channel widths of 20 and 10 μm . F-actin in a 20 μm channel undergoes random fluctuations consistent with unconfined F-actin in two dimensions, although F-actin in the 10 μm channel is occasionally deflected by the sidewalls of the channel and is flattened along the wall, as shown in Figure 1(c: second upper). In the 5 μm channel, however, this flattening effect is always observed. Figure 1(c: upper third) shows an S-shaped configuration of F-actin in the middle of transverse fluctuations. The confinement obviously affects F-actin configurations for $W \leq 5$ μm .

We introduce a simplified model to study the tangent-tangent correlation function of confined F-actin. We model the confined chains as two-dimensional wormlike chains, where the channel axis is in the \hat{x} direction and \hat{y} is the confined direction. We also assume that the chain is infinitely long and can be described by a function $\mathbf{r}(s)$, where s is the arclength along the chain. Further, we assume that the chain is confined by a harmonic potential in the \hat{y} direction with a spring constant k . The partition function is

$$Z = \int \mathbf{D}\vec{r} \delta[(\partial_s \vec{r})^2 - 1] e^{-\beta \int ds [1/2\kappa_0(\partial_s^2 \vec{r})^2 + 1/2k(r_y)^2]} \quad (3)$$

where $\beta \equiv 1/k_B T$ and the bending modulus $\kappa_0 \equiv k_B T L_p$.

In the high confinement limit, $\sin \theta \approx \theta$,¹⁴ where θ measures the angle from the x axis, and the model is completely solvable. The tangent-tangent correlation function is given by

$$\ln \langle C(s) \rangle \approx \frac{k_B T}{2(k\kappa_0^3)^{1/4}} e^{\frac{|s|}{\sqrt{2}} \left(\frac{k}{\kappa_0}\right)^{1/4}} \left\{ \cos \left[\frac{|s|}{\sqrt{2}} \left(\frac{k}{\kappa_0}\right)^{1/4} \right] - \sin \left[\frac{|s|}{\sqrt{2}} \left(\frac{k}{\kappa_0}\right)^{1/4} \right] \right\} - \frac{k_B T}{2(k\kappa_0^3)^{1/4}} \quad (4)$$

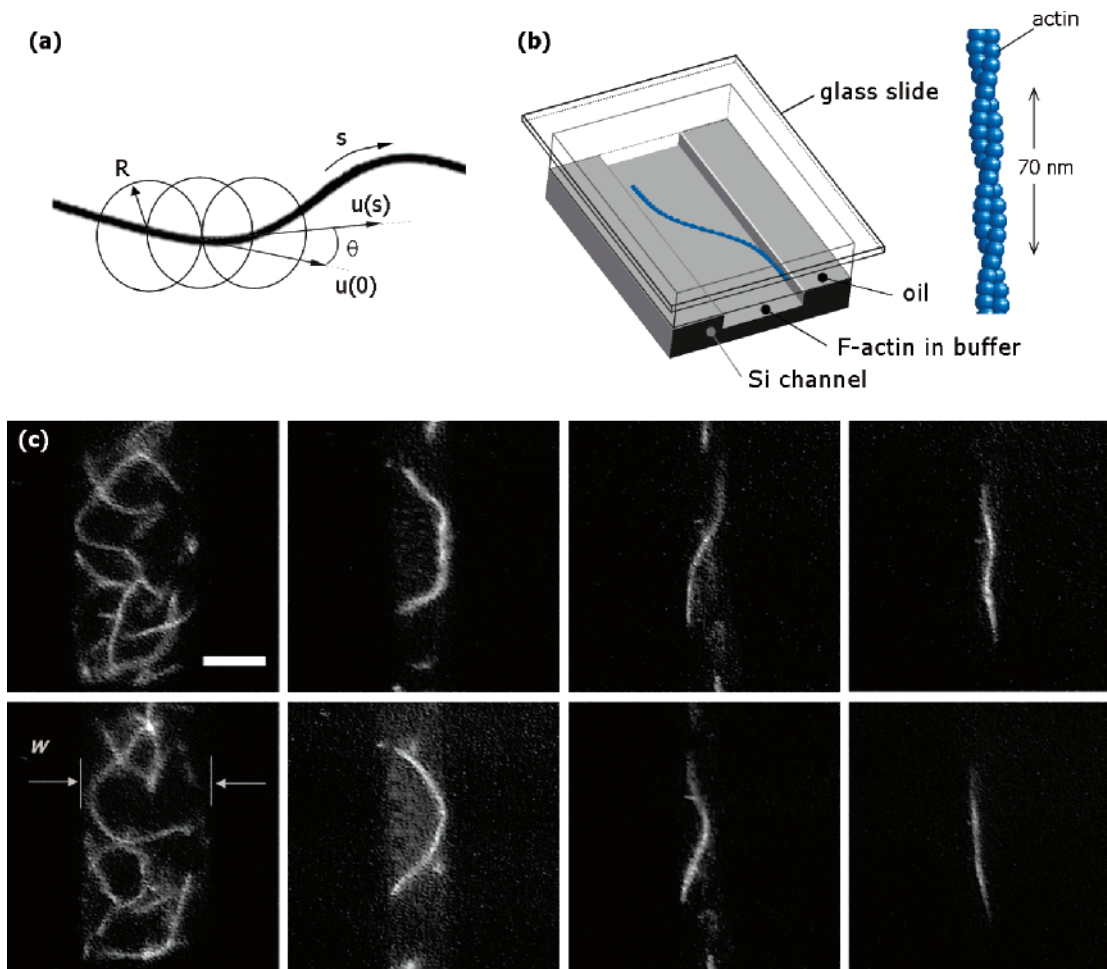


Figure 1. (a) Measurement of the tangent–tangent correlation function. (b) Graphic illustration of F-actin confined in microchannel. (c) Fluorescence video microscopy images of F-actin fluctuations in microchannels: from left to right, the channels are 20, 10, 5, and 3 μm wide, respectively, and 1 μm deep. Top and bottom images were taken in arbitrary time. Scale bar indicates 10 μm .

and the effective channel width W can be defined by $W^2 \equiv \langle r_y(0)r_y(0) \rangle = k_B T / 2(k^3 \kappa_0)^{1/4}$. The first minimum of the tangent–tangent correlation function in terms of W is

$$s_{\min} = \frac{\pi}{\sqrt{2}} W^{2/3} L_p^{1/3} \quad (5)$$

where L_p is the persistence length of the chain in two-dimensional free space. Additional minima in eq 4 are strongly suppressed. For the purpose of comparison with experiments, we take W to be the width of the microchannel.

The minimum, s_{\min} , has a natural interpretation as the contour distance between deflections of the filament due to the walls.⁹ At long distances, $\ln \langle C(s) \rangle \sim -(L_p/W)^{2/3} s$, signifying the presence of long-range orientational order induced by the confinement. Unfortunately, the F-actin appears too short to see this effect.

We measured $\langle C(s) \rangle$ from the fluorescence images for four different channel widths (Figure 2). Two correlation curves of $W = 20$ and 10 μm fall rapidly to zero, but those of the 3 and 5 μm channels never decrease below $\langle C(s) \rangle = 0.9$. Instead, they rise again, but fail to return to $\langle C(s) \rangle = 1$.

Equation 4 becomes $\ln \langle C(s) \rangle \approx -s/2L_p + O(s^2)$ for $s \ll s_{\min}$. To obtain the experimental persistence length of the chain, we fit the decaying portion of the experimental data to $\langle C(s) \rangle \sim e^{-s/2L_p^{\text{eff}}}$ as shown in Figure 2(b):

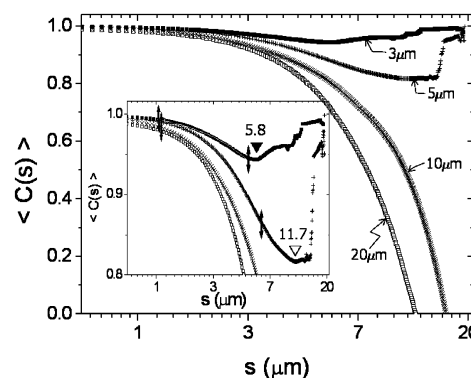


Figure 2. $\langle C(s) \rangle$ for $W = 3 \mu\text{m}$ (\blacksquare), $5 \mu\text{m}$ ($+$), $10 \mu\text{m}$ (\times), and $20 \mu\text{m}$ (\square). (Inset) L_p^{eff} were extracted by fitting the correlation curves to eq 2. Two cases, $W = 3$ and $5 \mu\text{m}$, are represented as examples. The double arrowed bars indicate the fitting region s_{fit} . In the 3 μm channel, for example, $1 \mu\text{m} \leq s_{\text{fit}} \leq 5 \mu\text{m}$, where 1 μm is the optical resolution limit of the fluorescence measurement.

inset). The measured values of L_p^{eff} are 5.9, 10.0, 29.3, and 38.2 μm for $W = 20, 10, 5,$ and $3 \mu\text{m}$, respectively. $L_p^{\text{eff}} = 5.9 \mu\text{m}$ at $W = 20 \mu\text{m}$ is similar to the persistence length measured in two-dimensional free space in other experiments,^{5,7–8} that is, $L_p^{\text{eff}}(W = 20 \mu\text{m}) \approx L_p$ in this study.

According to eq 5, for a semiflexible polymer under confinement, there exists a point s_{\min} at which the tangent–tangent correlation function attains a minimum. The theory gives the values of $s_{\min} = 8.4$ and $11.7 \mu\text{m}$ for $W = 3$ and $5 \mu\text{m}$, respectively, using the bare persistence length $L_p = 5.9 \mu\text{m}$ to determine κ_0 . In comparison, we experimentally measured s_{\min} from the correlation curves of Figure 2 and found $s_{\min} = 5.8$ and $11.7 \mu\text{m}$ for $W = 3$ and $5 \mu\text{m}$ (Figure 2 (inset)). However, there is no minimum in the case of the channels of width $W = 10$ and $20 \mu\text{m}$. We find good agreement between theory and experiment for $W = 5 \mu\text{m}$, but not for $W = 3 \mu\text{m}$. The reason for the inconsistency for the $3 \mu\text{m}$ channel is not yet clear, but one possibility is that the assumption of a two-dimensional polymer is increasingly inaccurate with decreasing channel width due to the effect of the channel depth. In particular, if d is the depth of the channel, it is necessary that $d \ll W$ for the theory to be valid.

In summary, we presented the first direct observation of the biaxial confinement of F-actin by a microchannel. With decreasing channel width, F-actin undergoes a transition from a 2D randomly oriented regime to a 1D biaxially confined regime with increasing L_p^{eff} . We found that the tangent–tangent correlation function of a semiflexible filament in a confinement regime shows a minimum, $s_{\min} = \pi W^{2/3} L_p^{1/3} \sqrt{2}$ with $W \leq L_p \leq s_{\min} < L_p^{\text{eff}}$, consistent with experiment.

Acknowledgment. C. D. Santangelo acknowledges useful discussions with F. MacKintosh, and M. C. Choi acknowledges discussions with J. Song. This work was supported by KISTEP I-03-064, KISTEP IMT-2000-B3-2, MOHW 0405-MN01-0604-0007, and partially by DMR 00-80034. C. R. Safinya and P. Pincus acknowledge support from NSF DMR-0503347. C. R. Safinya further acknowledges support from NSF CTS-0404444, ONR-N00014-05-1-0540, and DOE Office of Basic Energy Sciences contract W-7405-ENG-36 with the University of California. C. D. Santangelo acknowledges support by NSF DMR 0203755, NSF DMR01-29804, and a gift from Lawrence J. Bernstein.

Supporting Information Available: Details of calculation of the tangent–tangent correlation function for wormlike chains in two dimensions confined by a harmonic potential. Materials and experiment information on cleaning of Si microchannels, microinjector system InjectMan and Transjection 5346 (Eppendorf) mounted onto optical microscope (Nikon upright type Microphot-FX), and fluorescence microscopy system. This material is available free of charge via the Internet at <http://pubs.acs.org>.

References and Notes

- (1) Huxley, H. E. *Science* **1969**, *164*, 1356.
- (2) Condeelis, J. *Annu. Rev. Cell Biol.* **1993**, *9*, 411.
- (3) Stossel, T. P. *Science* **1993**, *260*, 1086.
- (4) *Molecular Cell Biology*; Lodish, H., Berk, A., Zipursky, L. S., Matsudaira, P., Baltimore, D., Darnell, J., Eds.; Freeman: San Francisco, 1999.
- (5) Riveline, D. C.; Wiggins, H.; Goldstein, R. E.; Ott, A. *Phys. Rev. E* **1997**, *56*, R1330.
- (6) Takebayashi, T.; Morita, Y.; Oosawa, F. *Biochim. Biophys. Acta* **1997**, *492*, 357.
- (7) Ott, A.; Magnasco, M.; Simon, A.; Libchaber, A. *Phys. Rev. E* **1993**, *48*, R1642.
- (8) Isambert, H.; Venier, P.; Maggs, A. C.; Fattoum, A.; Kassab, R.; Pantaloni, D.; Carlier, M. *J. Biol. Chem.* **1995**, *270*, 11437.
- (9) Odijk, T. *Macromolecules* **1983**, *16*, 1340.
- (10) G-actin, Alexa-Fluor 488 conjugate, was purchased from Molecular Probes Inc., Eugene, OR.; G-actin buffer, with 5 mM Tris-HCl, 0.2 mM CaCl₂, 0.5 mM ATP, and 0.2 mM DTT, was purchased from Cytoskeleton Inc., Denver, CO.
- (11) Pfohl, T.; Kim, J. H.; Yasa, M.; Miller, H. D.; Wong, G. C.; Bringezu, F.; Wen, Z.; Wilson, L.; Kim, M. W.; Li, Y.; Safinya, C. R. *Langmuir* **2001**, *17*, 5343.
- (12) Choi, M. C.; Pfohl, T.; Wen, Z.; Li, Y.; Kim, M. W.; Israelachvili, J. N.; Safinya, C. R. *Proc. Natl. Acad. Sci. U.S.A.* **2004**, *101*, 17340.
- (13) SIT camera purchased from Dage-MTI Inc., Michigan, IN.
- (14) We assume that the angle between the tangent vector of F-actin and the sidewall is small. To verify this, the angular distributions were measured. The distributions fit well with a Gaussian curve centered at 0° , -6.5° , with its fwhm at 16° , 19° , respectively, for $W = 3$ and $5 \mu\text{m}$. It can be interpreted that F-actin does not bend more than 8° (20°) from the sidewall of the $3 \mu\text{m}$ ($5 \mu\text{m}$) channel. However, in an unconfined regime (i.e., $W \geq 10 \mu\text{m}$), F-actin has a broad angular distribution between -70° and 50° .

MA051348N

Supplementary Materials

I. CONFINED WORMLIKE CHAINS

Here, we present the details of our calculation of the tangent-tangent correlation function for wormlike chains in two-dimensions confined by a harmonic potential. The wormlike chain model, introduced by Kratky and Porod [1], has an energy given by

$$\mathcal{H} = \frac{\kappa_0}{2} \int ds (\partial_s^2 \mathbf{r}), \quad (1)$$

subject to the constraint that $\partial_s \mathbf{r} = \hat{t}$, where $\mathbf{r}(s)$ is the vector that points to positions along the chain, \hat{t} is the unit tangent vector of the chain and s is the arclength along the chain. The quantity κ_0 is a material parameter given by $k_B T L_p$ where L_p is the persistence length of the chain, so named because it is the correlation length of the tangent vectors along the chain. In two dimensions, this problem takes on a particularly simple form using the substitution $\hat{t} = \cos \theta \hat{x} + \sin \theta \hat{y}$, with $\mathcal{H} = \int ds (\partial_s \theta)^2 / 2$.

We constrain the chain by adding a harmonic potential along the y direction

$$\mathcal{H}' = \frac{1}{2} k \int ds (\mathbf{r}(s) \cdot \hat{y})^2, \quad (2)$$

where k measures the amount of harmonic confinement of the chain. Now, the simple substitution, $\partial_s \mathbf{r} = \hat{t}$ is no longer possible. To proceed, we write the partition function

$$Z = \int \mathcal{D}\vec{r} \delta[(\partial_s \vec{r})^2 - 1] \exp \left\{ -\beta \int ds \left[\frac{1}{2} \kappa_0 (\partial_s^2 \vec{r})^2 + \frac{1}{2} k (r_y)^2 \right] \right\}, \quad (3)$$

where $r_y(s)$ is the y -component of the vector $\mathbf{r}(s)$.

Introducing an auxiliary field $\hat{t}(s)$, we notice that

$$1 = \int \mathcal{D}\hat{t} \delta[\hat{t}(s) - \partial_s \mathbf{r}(s)] = \int \mathcal{D}\hat{t} \mathcal{D}\vec{\omega} e^{i \int \vec{\omega}(s) \cdot [\hat{t}(s) - \partial_s \mathbf{r}(s)]}. \quad (4)$$

Integrating by parts in the second term in the exponential gives

$$1 = \int \mathcal{D}\hat{t} \mathcal{D}\vec{\omega} \exp \left[i \int \vec{\omega}(s) \cdot \hat{t}(s) + i \int ds \partial_s \vec{\omega} \cdot \mathbf{r}(s) + i \vec{\omega}(L) \cdot \mathbf{r}(L) - i \vec{\omega}(0) \cdot \mathbf{r}(0) \right], \quad (5)$$

for a chain that spans from $s = 0$ to $s = L$. For convenience in what follows, we assume periodic boundary conditions on the fields and take the limit that $L \rightarrow \infty$. Though real experimental chains are of finite length, we do not expect this simplification will change our fundamental conclusions about the tangent-tangent correlation function.

Substituting equation (5) into equation (3) and replacing all instances of $\partial_s \mathbf{r}$ with \hat{t} in equation (3), we find

$$Z = \int \mathcal{D}\mathbf{r} \mathcal{D}\vec{\omega} \mathcal{D}\hat{t} \delta[\hat{t}^2(s) - 1] \exp \left[-\beta \kappa_0 \int ds (\partial_s \hat{t})^2 / 2 - \beta k \int ds r_y^2(s) / 2 + i \int ds \vec{\omega} \cdot \hat{t} + i \partial_s \vec{\omega} \cdot \mathbf{r} \right]. \quad (6)$$

The integral over the x component of \mathbf{r} gives the constraint: $\partial_s \omega_x = 0$, which implies ω_x is a constant. The path integral over ω_x reduces to the constraint $\int ds \hat{t}_x$, which is just a restatement of the periodic boundary conditions of the chain. The integral over the r_y is a Gaussian integral, which gives

$$Z \propto \int \mathcal{D}\vec{\omega} \mathcal{D}\hat{t} \delta[\hat{t}^2(s) - 1] \exp \left[-\beta \kappa_0 \int ds (\partial_s \hat{t})^2 / 2 + i \int ds \omega_y(s) t_y(s) - \int ds (\partial_s \omega_y)^2 / (2\beta k) \right]. \quad (7)$$

We make the substitution $\hat{t} = \cos \theta \hat{x} + \sin \theta \hat{y}$, which automatically satisfies our constraint that $\hat{t}^2 = 1$. When the chain does not deviate strongly from the confinement axis, we have $\sin \theta \approx \theta$. Since the integral over ω_y is also Gaussian, it too can be performed. We find

$$Z \propto \int \mathcal{D}\theta \exp \left\{ -\frac{\beta L}{2} \sum_{q \neq 0} [\kappa_0 q^2 + k q^{-2}] |\theta_q|^2 \right\}, \quad (8)$$

where $\theta(s) = \sum_q \theta_q e^{iqs} \rightarrow L \int \frac{dq}{2\pi} \theta_q e^{iqs}$, in the infinite chain limit.

Now,

$$\langle \hat{t}(s) \cdot \hat{t}(0) \rangle = \langle e^{i[\theta(s) - \theta(0)]} \rangle = e^{-\frac{1}{2} \langle [\theta(s) - \theta(0)]^2 \rangle} = \exp[-\langle \theta(0)^2 \rangle + \langle \theta(s)\theta(0) \rangle]. \quad (9)$$

We immediately compute the correlation functions to be

$$\langle \theta(0)^2 \rangle = \frac{k_B T}{2\sqrt{2} (k\kappa_0^3)^{1/4}} \quad (10)$$

$$\langle \theta(s)\theta(0) \rangle = \frac{k_B T}{2\sqrt{2} (k\kappa_0^3)^{1/4}} \exp\left[-\frac{|s|}{\sqrt{2}} \left(\frac{k}{\kappa_0}\right)^{1/4}\right] \left\{ \cos\left[\frac{|s|}{\sqrt{2}} \left(\frac{k}{\kappa_0}\right)^{1/4}\right] - \sin\left[\frac{|s|}{\sqrt{2}} \left(\frac{k}{\kappa_0}\right)^{1/4}\right] \right\}. \quad (11)$$

and conclude that

$$\ln \langle \hat{t}(s) \cdot \hat{t}(0) \rangle = \frac{k_B T}{2\sqrt{2} (k\kappa_0^3)^{1/4}} \exp\left[-\frac{|s|}{\sqrt{2}} \left(\frac{k}{\kappa_0}\right)^{1/4}\right] \left\{ \cos\left[\frac{|s|}{\sqrt{2}} \left(\frac{k}{\kappa_0}\right)^{1/4}\right] - \sin\left[\frac{|s|}{\sqrt{2}} \left(\frac{k}{\kappa_0}\right)^{1/4}\right] \right\} - \frac{k_B T}{2\sqrt{2} (k\kappa_0^3)^{1/4}}. \quad (12)$$

II. MATERIALS AND EXPERIMENTS

A. Cleaning of Si microchannels

Si microchannels are cleaned by $\text{NH}_4\text{OH}:\text{H}_2\text{O}:\text{H}_2\text{O}_2$ (v:v:v=1:5:1) for 10 min at 80 °C, with rinsing in water ($\geq 18.2 \text{ M}\Omega \text{ cm}$). The water contact angle is $\theta_w < 5^\circ$ at a clean flat Si surface [2].

B. Microinjector system

InjectMan and Transjection5346 (Eppendorf) mounted onto optical microscopy (Nikon upright type Microphot-FX). The volume of the injected liquids is controlled by a compensation pressure with the step size 8 hPa in a range of 0 to 2000 hPa. Glass capillary tube with various tip shapes and diameters (0.5 - 20 μm in end diameter) are prepared with a micropipette puller P-97 (Sutter Instrument).

C. Fluorescence Microscopy system

To obtain high resolution fluorescence images, Nikon Diaphot 300 inverted scope, employing a 60x oil immersion objective with a 4x magnification lens is combined with a silicon intensified target (SIT) camera VE 1000 (Dage-MTI). For light source, we used 150W Xenon lamp (OPTIQUIP).

[1] O. Kratky and G. Porod, *Rec. Trav. Chim.* **68** (1949) 1106.

[2] T. Pfohl, J. H. Kim, M. Yasa, H. D. Miller, G. C. Wong, F. Bringezu, Z. Wen, L. Wilson, M. W. Kim, Y. Li, C. R. Safinya, *Langmir* **17** (2001) 5343; Choi, M. C.; Pfohl, T.; Wen, Z.; Li, Y.; Kim, M. W.; Israelachivili, J. N.; Safinya, C. R. *Proc. Natl. Acad. Sci. U.S.A.* **101** (2004) 17340.